IJE TRANSACTIONS B: Applications Vol. 31, No. 2, (February 2018) 382-393

International Journal of Engineering

Journal Homepage: www.ije.ir

# Modelling of Conventional and Severe Shot Peening Influence on Properties of High Carbon Steel via Artificial Neural Network

E. Maleki[a], G. H. Farrahi*[b]

[a] *Department of Mechanical Engineering, Sharif University of Technology-International Campus, Kish Island, Iran*
[b] *School of Mechanical Engineering, Sharif University of Technology, Tehran, Iran*

*PAPER INFO*

*Paper history:*
Received 10 June 2017
Received in revised form 05 August 2017
Accepted 08 September 2017

*Keywords*:
Artificial Neural Network
Severe Shot Peening
Residual Stress
Coverage
Almen Intensity

*ABSTRACT*

Shot peening (SP), as one of the severe plastic deformation (SPD) methods is employed for surface modification of the engineering components by improving the metallurgical and mechanical properties. Furthermore, artificial neural network (ANN) has been widely used in different science and engineering problems for predicting and optimizing in the last decade. In the present study, effects of conventional shot peening (CSP) and severe shot peening (SSP) on properties of AISI 1060 high carbon steel were modelled and compared via ANN. In order to networks training, the back propagation (BP) error algorithm is developed and data of experimental tests results are employed. Experimental data illustrates that SSP has superior influence over CSP to improve the properties. Different networks with different structures are trained with try and error process and the one which had the best performance is selected for modelling. Testing of the ANN is carried out using experimental data that they were not used during networks training. Distance from the surface (depth), SP intensity and coverage are regarded as inputs and microhardness, residual stress and grain size are gathered as outputs of the networks. Comparison of predicted and experimental values indicates that the networks are tuned finely and adjusted carefully and they have good agreement.

***doi**: 10.5829/ije.2018.31.02b.24*

## 1. INTRODUCTION

Most failures in engineering materials such as fatigue fracture are very sensitive to surface of materials, and in most cases failures originate from the surface layer of the components. Shot peening (SP) process is one of the known techniques that by severe plastic deformation (SPD) improves the surface properties, introducing a compressive residual stress in the surface layers of the material. This makes the nucleation and propagation of fatigue cracks more difficult. Shot peening is a process of cold working which increases the resistance of component [1-3]. The process involves the firing of hard balls under controlled velocity on to the critical zone of the surface of the component. The improvement in surface properties of the component is usually a consequence of the grain refinement, strain hardening of surface layers and induced compressive residual stresses [4]. Figure 1 demonstrates the schematic of shot peening process. Almen intensity and coverage among wide variety of known parameters are most influential in SP process. Severity of the SP is directly related to the value of the Almen intensity and coverage and it is classified into two cases of conventional shot peening (CSP) and severe shot peening (SSP). Common and high ranges of the mentioned parameters are used for CSP and SSP respectively [5]. Effective role of CSP and SSP process in improvement of the metallurgical and mechanical properties and fatigue behavior of the different materials were surveyed and confirmed experimentally by many works of researchers [6-10].

Artificial intelligence (AI) systems such as ANNs have been used efficiently to deal with a series of complex and nonlinear problems [11, 12]. In the complicated problems it is not easy to allocate them quantitatively as a function of the related parameters. In these cases ANN can be used to investigate and model the different problems for which quantitative

*Corresponding Author's Email: *farrahi@sharif.edu* (G. H. Farrahi)

Please cite this article as: E. Maleki, G. H. Farrahi, Modelling of Conventional and Severe Shot Peening Influence on Properties of High Carbon Steel via Artificial Neural Network, International Journal of Engineering (IJE), TRANSACTIONS B: Applications Vol. 31, No. 2, (February 2018) 382-393

evaluations are either lacking or not well formulated without any prior knowledge about parameters relations [13, 14].
Generally, ANN models learn from experimental data sets with specific input and output parameters to generalize the suitable patterns [15, 16].

The aim of the present study is to model the effects of both CSP and SSP processes on properties of AISI 1060 high carbon steel. Therefore, at first, eight different SP treatments, with different Almen intensity and coverage, including CSP and SSP were applied experimentally. Microstructure of the treated specimens were characterized using scanning electron microscopy (SEM), field emission scanning electron microscopy (FESEM), high resolution transmission electron microscope (HRTEM) observations and X-ray diffraction (XRD) analysis. Also, mechanical properties were characterized using microhardness and residual stress measurement. The comparison of the conventional and severe shot peened specimens has been conducted within the context of above measurements. The experimental results indicate that the SSP have superior effect to improve the properties than CSP. After obtaining experimental results, distribution of the three parameters of microhardness, residual stress and grain size in depth were modeled and investigated via ANN. Depth, Almen intensity and coverage were considered as inputs of ANN modelling in this study.

## 2. EXPERIMENTAL PROCEDURE

AISI 1060 high carbon steel is employed as specimens' material in this study. Chemical composition of the material is presented in Table 1.

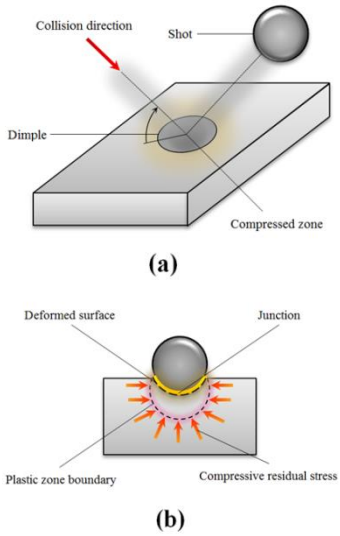


**Figure 1.** Schematic of (a) shot peening process and (b) plastic deformation caused by SP

AISI 1060 is widely used in mechanical engineering components, tools and railway wheels [17, 18].

Specimens were quenched from 850ºC in oil, tempered at 300ºC for 1 h and ground. After preparation of the specimens, they were shot peened from conventional to severe, using air blast shot peening device. Almen intensity was determined according to SAE J443 standard [19]. Table 2 shows the effective parameters of accomplished SP treatments. Microstructure observations were carried out via VEGA\\TESCAN-XMU scanning electron microscope (SEM) and field emission scanning electron microscopy (FESEM) using Mira 3-XMU. Specimens were etched by 2% Nital before microscope observation.

In order to achieve the specimens' grain size after SP treatments, X-ray diffraction (XRD) measurements and high resolution transmission electron microscope (HRTEM) were applied. In the XRD analysis width of the diffraction peak at half the maximum intensity (FWHM) and crystallite size were measured on the surface of the specimens. For the XRD analysis, X'Pert PRO MPD (PANalytical ) X-ray diffractometer system and X'Pert High Score Plus (V. 3) analyzer is employed with Cu Kα radiation operated at 40 kV and 40 mA, scanning angle of 30º–150º and irradiated area of 10 mm. For HRTEM observations, samples were prepared by ion polishing to a thickness of 60 µm by disc grinding and to about 5 µm by dimple grinding from metal side. Specimens were evaluated via a JEOL JEM 2100 High Resolution Transmission Electron Microscope operated at 200 kV. The peened samples were mechanically cross sectioned, polished and mounted on copper grids for TEM observation. The distance of a given observed region from the free surface was measured in the TEM using low magnification imaging. The mean grain size was evaluated from layers within a vertical range of 10 µm. The total counts for each size measurement was at least above 75.

Microhardness measurements were performed on a Qness GmbH Q10 microhardness tester at a load of 10 gf with duration of 8 s using Vickers indenter on the surface and in depth up to 400 µm to obtain the related profile. Residual stresses were measured using Xstress 3000 G2/G2R X-ray Stress Analyzer (radiation Cr Kα, irradiated area of 4 mm diameter, diffraction angle (2θ) ~156º and ψ scanned between 45 and -45º). Measurements were accomplished in depth by removing a very thin layer of material (~ 20 µm) through electro-polishing with a solution of acetic acid (94%) and perchloric acid (6%).

## 3. ARTIFICIAL NEURAL NETWORK

ANNs, as highly interconnected arrays of processing computational nodes (neurons) which its basis has been

**TABLE 1.** Chemical composition of AISI 1060 high carbon steel (weight %).

| C | Si | S | P | Mn | Ni | Cr | Mo | Fe |
|---|---|---|---|---|---|---|---|---|
| 0.57-0.65 | Max 0.40 | Max 0.035 | Max 0.035 | 0.60-0.90 | Max 0.40 | Max 0.40 | Max 0.10 | Bal. |

**TABLE 2.** Effective parameters of accomplished SP treatments

| Treatment No. | Shot | Shot diameter (mm) | Air pressure (bar) | Almen intensity (0.0001 in. A) | Surface coverage (%) | SP treatment type |
|---|---|---|---|---|---|---|
| 1 | S 280 | 0.7 | 3 | 17 | 100 | CSP |
| 2 | S 280 | 0.7 | 3 | 17 | 700 | SSP |
| 3 | S 280 | 0.7 | 3 | 17 | 1500 | SSP |
| 4 | S 280 | 0.7 | 5 | 21 | 100 | CSP |
| 5 | S 280 | 0.7 | 5 | 21 | 700 | SSP |
| 6 | S 280 | 0.7 | 5 | 21 | 1500 | SSP |
| 7 | S 280 | 0.7 | 5 | 21 | 2000 | SSP |
| 8 | S 330 | 0.8 | 5 | 25 | 100 | CSP |

inspired by human's brain, have been widely used and have proven to be flexible interpolation functions that are in principle able to adapt to fit any complex database and have power of prediction and optimization [20]. Circumstance of modelling via ANN with considering the performance of the biological and artificial neurons was studied in many works [21]. An artificial neuron is presented in Figure 2. A single neuron computes the sum of the entered inputs which are multiplied with a variant called the weight, adds a bias term, and drives the result through a transfer function to produce a single output. Generally, linear, tangent sigmoid (Tansig) and logarithmic sigmoid (Logsig) functions are used as the popular transfer functions. The mentioned transfer functions are determined as follows:

$$Linear: \chi(x) = linear(x) \quad (1)$$

$$Tansig: \phi(x) = \frac{2}{1+e^{-2x}} - 1 \quad (2)$$

$$Logsig: \psi(x) = \frac{1}{1+e^{-x}} \quad (3)$$

Structurally, every ANN is made up input layer, hidden layer/layers and output layer [22]. The structure of an ANN model is determined by the number of its layers and respective number of nodes in each layer and the nature of the transfer function [23]. Architecture of a neural network that feeds with r and s input p and output a parameters respectively, whit weight matrixes w, bias vectors b, linear combiner u and transfer function f, is demonstrated in Figure 3.

**3. 1. Modelling via ANN** In order to model a process via ANN, two main steps of network training and testing must be considered. The main difference between these two networks is the used data sets; employed data set for testing was not used during training. Training process is necessary to achieve the optimal network structure and the related parameters. However, testing process is essential for performance assessment of the trained network.

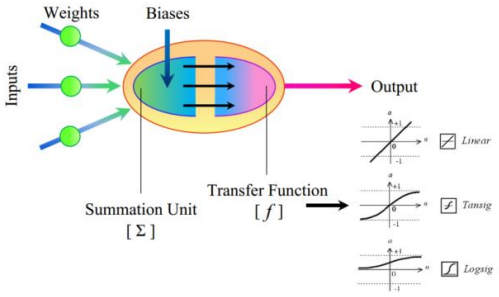


**Figure 2.** Schematic of an artificial neuron

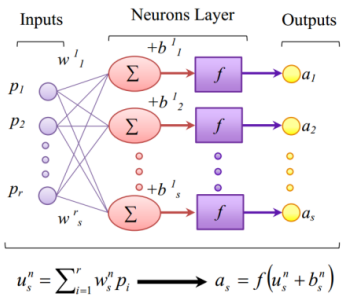


**Figure 3.** One layer network that feed with r inputs and s outputs

**3. 2. Training process** The process of calculation of weights and biases values with adaptation, learning from and evaluating of training patterns is training. Sets of known input and output data is used to train the network. In order to obtain optimal structure (OS) of ANN with highest performance and least errors there is no suitable formula.

Therefore, one of the challenging steps in ANN modelling is selecting the optimal architecture via trial and error [24, 25]. Usually, this procedure is carried out by training different networks with different structures and comparing them till to gain the acceptable ranges of error. In this study, the feed-forward error back-propagation (BP) algorithm is used to train the networks that are using a gradient descent technique to minimize the error for particular training pattern.

**3. 2. 1. Implementation of ANN** In the present study, the three effects of SP process on surface properties of AISI 1060 high carbon steel, such as hardness, residual stress and grain size were simulated for each accomplished treatments. Various networks with different structures were trained to obtain the OS. Distance from the surface (depth), SP intensity and coverage are regarded as inputs and microhardness, residual stress and grain size are gathered as outputs of the networks. Figure 4 displays the schematic of ANN structure with four layers and feed-forward with BP algorithm that all the neurons are fully interconnected.

Values of depth, SP intensity and coverage are logged into input layer to estimate the values of microhardness, residual stress and grain size. In this study the parameters of shot size and air pressure are can be considered as an in inputs either, instead of the Almen intensity. But, in order to increase the accuracy of the results, the parameter of Almen intensity is selected that cover the effects of both shot size and air pressure.

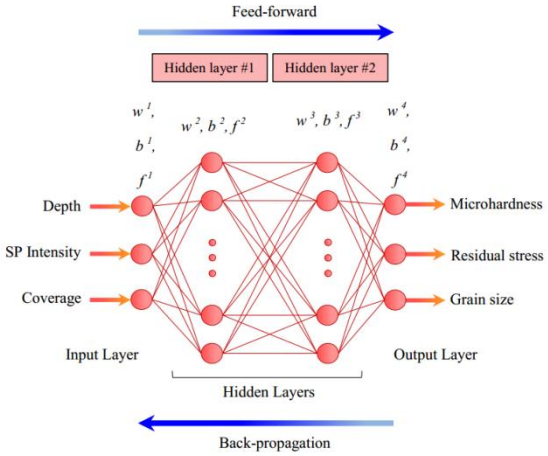


**Figure 4.** Conceptual structure of ANN according to the considered input and output parameters of the network

**3. 3. Performance Evaluation of ANN** The efficiency of the developed ANN models in this study were assessed using several statistical criteria by comparison between experimental and obtained predicted results of ANN. Four criteria of coefficient of correlation (R2), root mean square error (RMSE), mean relative error (MRE) and mean absolute error (MAE). The criteria have been calculated by following equations:

$$R^2 = \frac{\sum_{i=1}^{n}\left(f_{EXP,i} - F_{EXP}\right)\left(f_{ANN,i} - F_{ANN}\right)}{\sqrt{\sum_{i=1}^{n}\left(\left(f_{EXP,i} - F_{EXP}\right)^2\left(f_{ANN,i} - F_{ANN}\right)^2\right)}} \quad (4)$$

$$RMSE = \sqrt{\frac{\sum_{i=1}^{n}\left(f_{EXP,i} - f_{ANN,i}\right)^2}{n}} \quad (5)$$

$$MRE = \frac{1}{n}\sum_{i=1}^{n}\frac{\left|f_{EXP,i} - f_{ANN,i}\right|}{f_{EXP,i}} \times 100 \quad (6)$$

$$MAE = \frac{1}{n}\sum_{i=1}^{n}\left|f_{EXP,i} - f_{ANN,i}\right| \quad (7)$$

where n is the number of used sample for modelling, fEXP is the experimental value and fANN is the networks predicted value. Also, the values of FEXP and FANN are calculating as follows:

$$F_{EXP} = \frac{1}{n}\sum_{i=1}^{n} f_{EXP,i} \quad (8.a)$$

$$F_{ANN} = \frac{1}{n}\sum_{i=1}^{n} f_{ANN,i} \quad (8.b)$$

**3. 4. Generating Model Function** After accomplishing successful training and achieving the OS, the values of weights and biases for each layer were obtained. Finally, the model function that explains the relations of regarded input and output parameters can be determined as follows:

$$a^1 = f^1(w^1 i + b^1) \quad (9.a)$$

$$a^2 = f^2(w^2 i\,1 + b^2) \quad (9.b)$$

$$a^3 = f^3(w^3 i^2 + b^3) \quad (9.c)$$

$$a^4 = f^4(w^4 i^3 + b^4) \quad (9.d)$$

$$M(m(1), m(2), m(3)) = a^4 = f^4(w^4 f^3\,(w^3 f^2(w^2 f^1(w^1 i + b^1) + b^2) + b^3) + b^4) \quad (10)$$

where $a^1$, $a^2$ and $a^3$ are outputs of the first, second and third layer, respectively; a4 is the fourth layer output which is equal to the function M(m(1), m(2), m(3). The function M collects the values of three input parameters

of depth, SP intensity and coverage that they fed to the network. The desired outputs of microhardness, residual stress and grain size depicted with m(1), m(2) and m(3) respectively .

**3. 5. Used methodology of ANN** The methodology of ANN is stated according to the convergence of errors criteria. The basis of the used method in this study is the value of R2, although the other values of statistical criteria such as RMSE [26], MSE [20, 27] and ME [28] can be employed as the foundation of the ANN developing approach. R2 is a measure of correlation which is widely used as a rate of the degree of linear dependence between two variables. Based on the results reported by Elangovan et al. [29] and Maleki et el. [22, 30, 31], attaining values of R2 more than 0.99 are much acceptable for this criterion (The absolute values of R2 are less than or equal to 1). The methodology used for neural network application is shown in Figure 5.

## 4. RESULTS AND DISCUSSIONS

As it was mentioned, in order to characterize the microstructure of the specimens different microscopic observations were performed.

Figure 6 presents the SEM images of as-received and shot peened specimens with Almen intensity of 21A at different coverage of 100, 700 and 1500 %. It can be observed from SEM micrographs that by increasing the severity of SP process via increasing of coverage, grains size and spaces between the grains boundaries are decreased.

The cross-sectional FESEM observations of the treated specimen with different Almen intensities of 17, 21 and 25 A at two coverages of 100 and 1500% are illustrated in Figure 7. In the CSP treatments (treatments with 100% coverage) the ultrafine grained layer is generated beneath the top surface and also work-hardened layers can be observed as well.

However, in the SSP treatments (treatments with 700, 1500 and 2000% coverage) distinct region separated with sharp boundaries from the underlying plastically deformed and work-hardened layer is clearly recognized on the top surface.

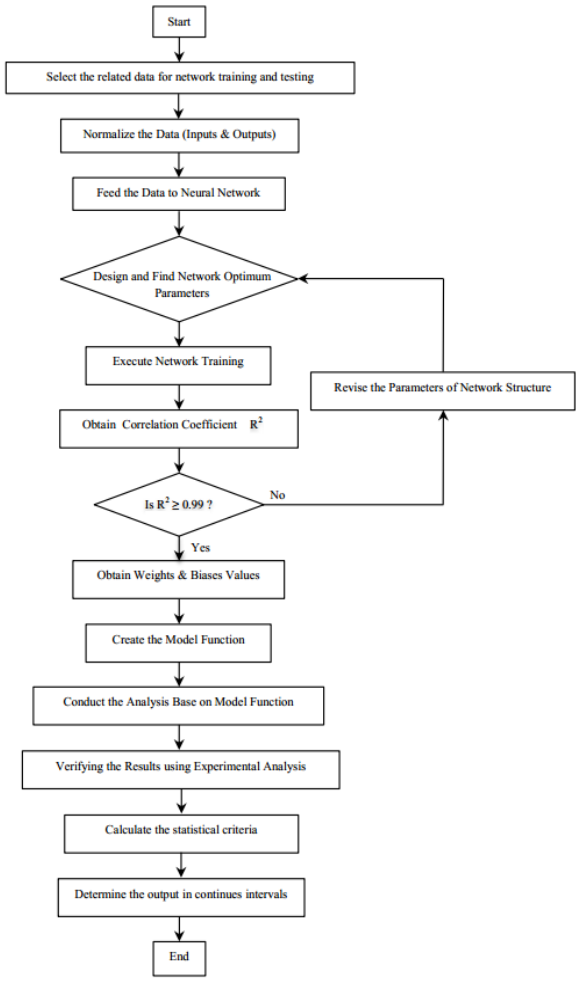


**Figure 5.** The used methodology consisting of network training, investigation of the results achieved from ANN and results evaluation

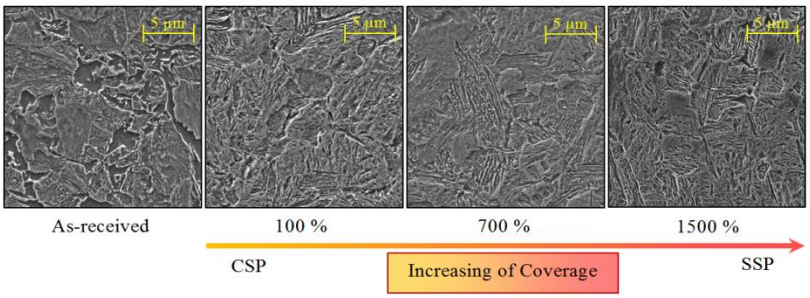


**Figure 6.** SEM observations of the as-received and shot peened specimens with Almen intensity of 21 A and different coverages of 100, 700 and 1500%

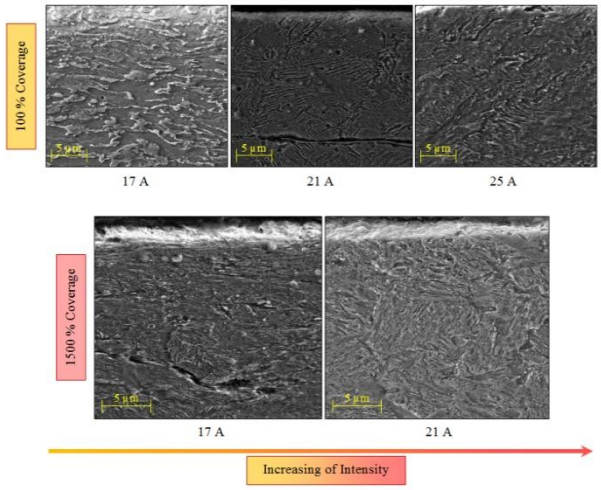


**Figure 7.** FESEM observations of the shot peened specimens with different Almen intensities of 17, 21 and 25 A and different coverages of 100 and 1500%

This layer, representing a very dense structure near the surface, as reported by Saitoh et al. [32], is considered to be the fine grained layer.

Also, very thin layer of UFG were seen under the sharp boundary of severe shot peened specimens. Figure 8 shows the XRD patterns of the surface of severe shot peened specimens. The grain sizes of the related specimens are determined using Scherer's equation. The application of XRD for obtaining the full width at half maximum (FWHM) to obtain grain size are limited to nano-scale particles. However, if the grains size is larger than about 100 nm the HRTEM (or TEM) gives more precise grain size distributions [33]. Therefore, grain size of the specimens that treated with CSP processes was determined via HRTEM observations. Figure 9 depicts the HRTEM observations of the conventional shot peened specimens with different considered Almen intensities. HRTEM images clearly reveal that the higher the intensity is, the smaller the grain size is. In the present study as it aforementioned, obtained results from the accomplished specimens were used to develop the ANN for modelling of SP process. The values of microhardness, residual stress and grains size in every 60 µm intervals from the surface to depth of 420 µm were achieved. The reason for selection of 0-420 µm from the surface is that the most of the variations in the values of mentioned parameters usually (microhardness, residual stress and grains size) occur in this range. Experimental results (Table 3) revealed that increasing both Almen intensity and coverage enhanced the properties of the specimens, but as it observed the effect of increasing Almen intensity is more than the influence of raising coverage level in the same conditions. The microhardness measurements, depicted that hardness of the surface of the severe shot peened specimens have been enhanced remarkably. Both of the CSP and SSP processes induced compressive residual stresses on the surface of specimens and by increasing the Almen intensity and coverage the value of compressive residual stress is enhanced.

As it is shown in Table 3, 64 experimental test results of CSP and SSP processes on AISI 1060 high carbon steel have been employed for training and testing of the networks. In order to cover the whole range of the used data in the both training and testing process, the testing samples were selected from each values of depth, Almen intensity and coverage. 48 samples data (75%) were employed as data sets for network training. In the network testing, 16 different samples data (25%) which were not used during training were considered. Various networks were trained to achieve the OS for generating the correspondence model function. Related information of 15 different trained networks with trial and error approach for modelling of microhardness is shown in Table 4.

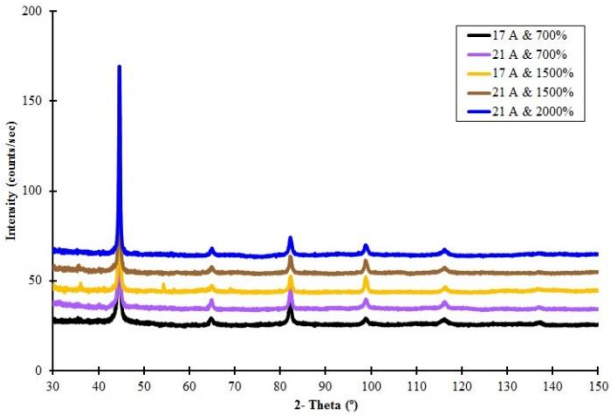


**Figure 8.** Intensity distribution of severely treated specimens

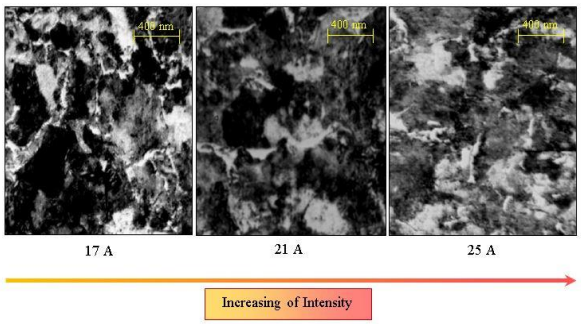


**Figure 9.** Bright-field HRTEM images of the shot peened specimens with CSP treatment with Almen intensities of 17, 21 and 25 A

**TABLE 1.** Results of experimental tests on 64 different samples

| Sample No. | Depth (μm) | Almen intensity (0.001 in A) | Surface coverage (%) | Microhardness (Hv) | Residual stress (MPa) | Grain size (nm) | Sample type |
|---|---|---|---|---|---|---|---|
| 1 | 0 | 17 | 100 | 355 | -221 | 515 | Testing |
| 2 | 0 | 17 | 700 | 411 | -267 | 82 | Training |
| 3 | 0 | 17 | 1500 | 480 | -291 | 48 | Training |
| 4 | 0 | 21 | 100 | 389 | -292 | 460 | Training |
| 5 | 0 | 21 | 700 | 463 | -327 | 52 | Training |
| 6 | 0 | 21 | 1500 | 547 | -314 | 45 | Training |
| 7 | 0 | 21 | 2000 | 561 | -339 | 42 | Training |
| 8 | 0 | 25 | 100 | 401 | -318 | 410 | Testing |
| 9 | 60 | 17 | 100 | 343 | -273 | 560 | Training |
| 10 | 60 | 17 | 700 | 394 | -314 | 100 | Testing |
| 11 | 60 | 17 | 1500 | 447 | -350 | 66 | Training |
| 12 | 60 | 21 | 100 | 372 | -325 | 532 | Training |
| 13 | 60 | 21 | 700 | 440 | -369 | 77 | Training |
| 14 | 60 | 21 | 1500 | 514 | -391 | 53 | Training |
| 15 | 60 | 21 | 2000 | 531 | -467 | 46 | Testing |
| 16 | 60 | 25 | 100 | 387 | -399 | 460 | Training |
| 17 | 120 | 17 | 100 | 323 | -173 | 800 | Training |
| 18 | 120 | 17 | 700 | 363 | -404 | 151 | Training |
| 19 | 120 | 17 | 1500 | 422 | -480 | 90 | Testing |
| 20 | 120 | 21 | 100 | 341 | -339 | 670 | Training |
| 21 | 120 | 21 | 700 | 421 | -452 | 121 | Training |
| 22 | 120 | 21 | 1500 | 470 | -545 | 72 | Testing |
| 23 | 120 | 21 | 2000 | 482 | -599 | 58 | Training |
| 24 | 120 | 25 | 100 | 352 | -391 | 740 | Training |
| 25 | 180 | 17 | 100 | 304 | -139 | 1700 | Training |
| 26 | 180 | 17 | 700 | 323 | -352 | 750 | Training |
| 27 | 180 | 17 | 1500 | 381 | -511 | 189 | Training |
| 28 | 180 | 21 | 100 | 319 | -275 | 1300 | Testing |
| 29 | 180 | 21 | 700 | 369 | -420 | 700 | Testing |
| 30 | 180 | 21 | 1500 | 383 | -541 | 160 | Training |
| 31 | 180 | 21 | 2000 | 392 | -560 | 101 | Training |
| 32 | 180 | 25 | 100 | 331 | -347 | 1410 | Training |
| 33 | 240 | 17 | 100 | 295 | -121 | 3800 | Training |
| 34 | 240 | 17 | 700 | 311 | -324 | 2500 | Training |
| 35 | 240 | 17 | 1500 | 320 | -479 | 1200 | Training |
| 36 | 240 | 21 | 100 | 295 | -210 | 3100 | Testing |
| 37 | 240 | 21 | 700 | 320 | -366 | 2000 | Testing |
| 38 | 240 | 21 | 1500 | 343 | -450 | 600 | Training |
| 39 | 240 | 21 | 2000 | 402 | -536 | 510 | Training |
| 40 | 240 | 25 | 100 | 297 | -301 | 2800 | Training |
| 41 | 300 | 17 | 100 | 290 | -100 | 6800 | Training |
| 42 | 300 | 17 | 700 | 294 | -322 | 4700 | Training |
| 43 | 300 | 17 | 1500 | 290 | -466 | 2500 | Testing |
| 44 | 300 | 21 | 100 | 290 | -210 | 6000 | Training |
| 45 | 300 | 21 | 700 | 301 | -366 | 4500 | Training |
| 46 | 300 | 21 | 1500 | 314 | -450 | 2100 | Testing |
| 47 | 300 | 21 | 2000 | 356 | -484 | 2200 | Training |
| 48 | 300 | 25 | 100 | 291 | -281 | 5700 | Training |
| 49 | 360 | 17 | 100 | 289 | -109 | 7770 | Training |
| 50 | 360 | 17 | 700 | 283 | -300 | 7000 | Testing |
| 51 | 360 | 17 | 1500 | 299 | -430 | 3800 | Training |
| 52 | 360 | 21 | 100 | 287 | -195 | 7510 | Training |
| 53 | 360 | 21 | 700 | 303 | -348 | 6500 | Training |
| 54 | 360 | 21 | 1500 | 309 | -441 | 5000 | Training |
| 55 | 360 | 21 | 2000 | 327 | -500 | 4100 | Testing |
| 56 | 360 | 25 | 100 | 294 | -238 | 6800 | Training |
| 57 | 420 | 17 | 100 | 290 | -32 | 9100 | Testing |
| 58 | 420 | 17 | 700 | 287 | -258 | 8100 | Training |
| 59 | 420 | 17 | 1500 | 300 | -370 | 7000 | Training |
| 60 | 420 | 21 | 100 | 281 | -149 | 8950 | Training |
| 61 | 420 | 21 | 700 | 290 | -304 | 7800 | Training |
| 62 | 420 | 21 | 1500 | 301 | -439 | 6600 | Training |
| 63 | 420 | 21 | 2000 | 308 | -484 | 6200 | Training |
| 64 | 420 | 25 | 100 | 298 | -187 | 8200 | Testing |

As it is shown, the structure of the ANN modellings are stated from simple to complex and as more the complexity of the networks structure is, the higher the rate of training to balance the speed of training process will be. The average CPU time for each accomplished ANN modelling is about 21 min, that is computed using a computer equipped with a core i7- Q740 processor running at 1.73 GHz and 4.00 GB of RAM. The reason behind high CPU processing time is the number of used data for training (64 samples data) and intricacy of the SP process that was made the generating of related model function too difficult. After investigation of the trained network, ANN modelling number 13 with architecture of the 3×24×24×3 that has the highest value of R2 and the least values of RMSE, MRE and MAE is selected as an OS to generate the model function. Figures 10 and 11 show the comparative diagrams of predicted and experimental values for both training and testing samples for all of the considered networks output parameters.

Figure 12 depicts the relative error (RE) values of considered output parameters of ANN for training and testing samples. According to the results, the maxim values of RE for training and testing samples are 2.94 (sample 7) and 1.81% (sample 28), respectively, both of which are related to the residual stress and are acceptable.

Based on the evaluation of the ANN via mentioned statistical criteria for both training and testing data sets, the relevant information of employed network are shown in Table 5.

**TABLE 4.** Related information of 15 different networks for modelling of microhardness

| ANN Modelling No. | Rate of Training | Layers Structure | Hidden Transfer Function | Output Transfer Function | $R^2$ | RMSE | MRE (%) | MAE |
|---|---|---|---|---|---|---|---|---|
| 1 | 0.110 | 3×6×9×3 | Logsig | Linear | 0.9702 | 0.0146 | 1.1394 | 0.0121 |
| 2 | 0.110 | 3×6×12×3 | Tansig | Linear | 0.9731 | 0.0140 | 1.1301 | 0.0117 |
| 3 | 0.120 | 3×9×12×3 | Logsig | Logsig | 0.9788 | 0.0132 | 1.1222 | 0.0109 |
| 4 | 0.120 | 3×9×18×3 | Tansig | Linear | 0.9812 | 0.0127 | 1.0796 | 0.0100 |
| 5 | 0.120 | 3×12×12×3 | Logsig | Tansig | 0.9853 | 0.0120 | 0.9575 | 0.0093 |
| 6 | 0.125 | 3×12×15×3 | Logsig | Logsig | 0.9884 | 0.0113 | 0.9108 | 0.0084 |
| 7 | 0.130 | 3×15×15×3 | Tansig | Linear | 0.9926 | 0.0095 | 0.8299 | 0.0070 |
| 8 | 0.125 | 3×15×18×3 | Tansig | Linear | 0.9941 | 0.0084 | 0.7989 | 0.0063 |
| 9 | 0.145 | 3×18×21×3 | Logsig | Tansig | 0.9975 | 0.0078 | 0.7445 | 0.0056 |
| 10 | 0.145 | 3×21×18×3 | Logsig | Tansig | 0.9989 | 0.0070 | 0.6992 | 0.0049 |
| 11 | 0.150 | 3×21×21×3 | Logsig | Logsig | 0.9992 | 0.0066 | 0.6762 | 0.0046 |
| 12 | 0.155 | 3×21×24×3 | Logsig | Tansig | 0.9997 | 0.0061 | 0.6000 | 0.0040 |
| **13** | **0.160** | **3×24×24×3** | **Logsig** | **Logsig** | **0.9998** | **0.0054** | **0.5878** | **0.0038** |
| 14 | 0.165 | 3×24×27×3 | Logsig | Tansig | 0.9998 | 0.0058 | 0.5994 | 0.0039 |
| 15 | 0.165 | 3×27×27×3 | Logsig | Logsig | 0.9996 | 0.0063 | 0.6013 | 0.0041 |

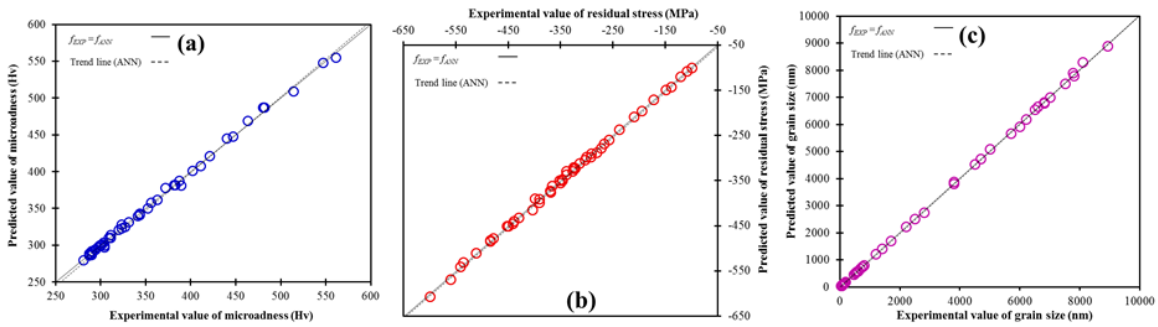


**Figure 10.** Comparison of the predicted (ANN response) and experimental values for each 48 training samples for (a) microhardness, (b) residual stress and (c) grain size

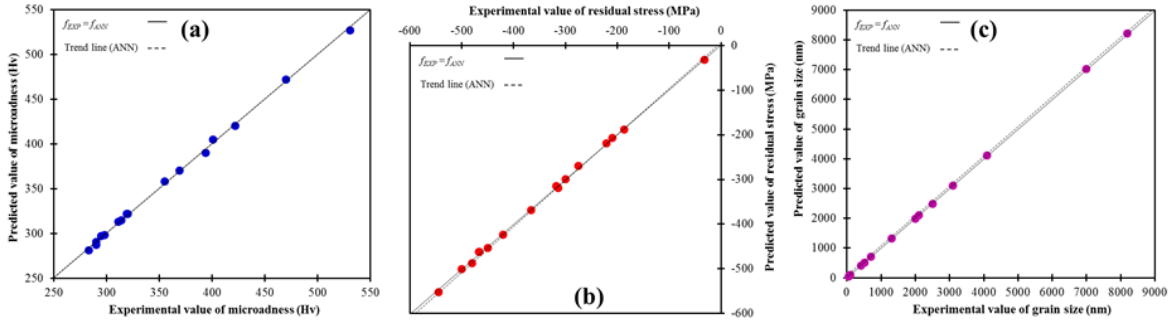


**Figure 11.** Comparison of the predicted (ANN response) and experimental values for each 16 testing samples for (a) microhardness, (b) residual stress and (c) grain size

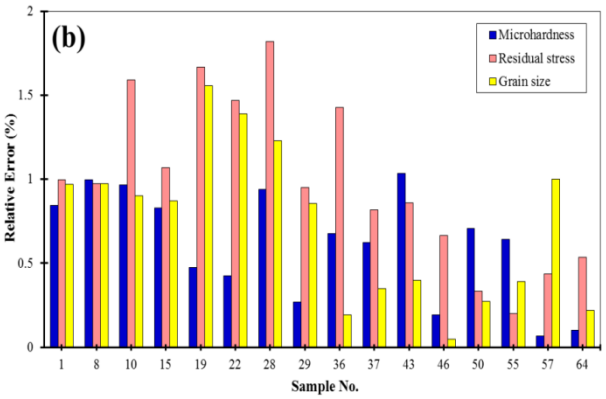


**Figure 12.** Values of relative errors obtained for (a) training data set (b) testing data set

According to the results in network training, it is observed that the values of R2 are more than 0.999, the RMSE, MRE and MAE values are very close to 0 and in very small range (RMSE: [0.0047-0.0069]), MRE: [0.5878-0.8970] and MAE: [0.0022-0.0050]) for all of the regarded output parameters of SP process effects.Therefore, it is concluded that networks are finely trained and carefully adjusted.

Likewise, in network testing the values of R2 are more than 0.999. Values of R2 for networks testing have negligible reduction in comparison with networks training. Moreover values of RMSE, MRE and MAE for networks testing are in tiny range as well (RMSE: [0.0027-0.0070], MRE: [0.6122-0.9886]) and MAE: [0.0013-0.0058]), and they are acceptable. The maximum value of errors for both networks training and testing are related to the residual stress. Totally, based on the results of the statistical criteria it can be seen that the obtained error values in the accomplished modelling is less than 1% .

In simulation of each output parameters, some mutations are seen in errors of different samples. The reason for this phenomenon is the inability of the neural network, which was trained by the error back propagation algorithm, to converge while simulating data in a wider range.

Variations of microhardness, residual stress and grain size from the shot peened surface to the bulk material are shown in Figure 13 which is achieved by generated model functions of used ANN optimum structures in this paper.

The important point observed in the diagrams of Figure 13 is very high match in discontinuous (spot form) experimental values and continuous predicted values in the sudden jumps and variations of concavity of experimental values trends.

Based on the results, it can be concluded that when the ANNS are adjusted finely, the modelling results are in acceptable agreement with the experimental results.

**TABLE 2.** Obtained values of $R^2$, RMSE, MRE and MAE for trained and tested network

| Output parameter | Network Training | | | | Network Testing | | | |
|---|---|---|---|---|---|---|---|---|
| | $R^2$ | RMSE | MRE (%) | MAE | $R^2$ | RMSE | MRE (%) | MAE |
| Microhardness | 0.9998 | 0.0054 | 0.5878 | 0.0038 | 0.9997 | 0.0045 | 0.6122 | 0.0039 |
| Residual stress | 0.9996 | 0.0069 | 0.8970 | 0.0050 | 0.9994 | 0.0070 | 0.9886 | 0.0058 |
| Grain size | 0.9998 | 0.0047 | 0.6630 | 0.0022 | 0.9998 | 0.0027 | 0.7263 | 0.0013 |

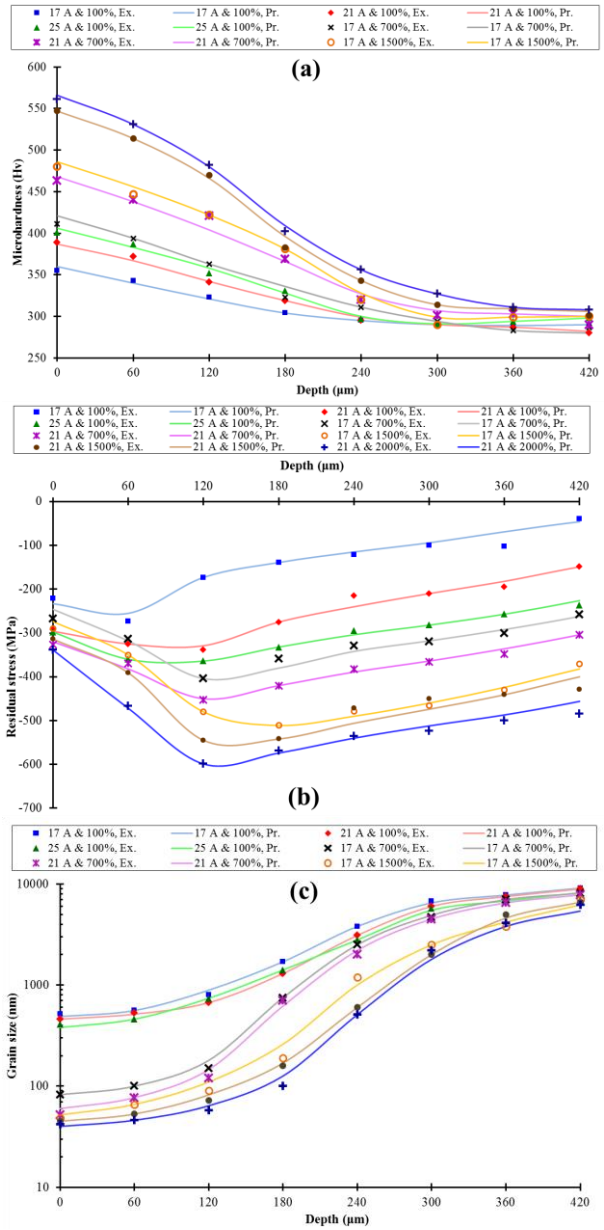


**Figure 13.** Predicted values of ANN using optimum structure and obtained model function for Simulation of (a) microardness, (b) residual stress and (c) grain size

## 5. CONCLUSION

In the present study, the AISI 1060 carbon steel specimens have been shot peened to improve the mechanical and metallurgical properties. Eight different shot peening treatments with 17, 21 and 25 A Almen intensities with coverage of 100, 700, 1500 and 2000% were applied. Properties of treated specimens were investigated through various experimental approaches. The experimental results reveal that in the SSP the grains in the surface layer became nanostructured. Both CSP and SSP processes induced compressive residual stresses on the shot peened surface. Increasing the severity of shot peening by both Almen intensity and coverage as main parameters of the shot peening process enhances metallurgical and mechanical properties of the components. Although the Almen intensity is more influential than the coverage under the same conditions. Three parameters of microhardness, residual stress and grain size, which can be affected by SP process, were also modeled via ANN. Results of the developed network indicate that the values of $R^2$ are more than 0.999 and the other statistical errors are in very small range and less than 1% that they are acceptable. The predicted values of microhardness, grain size and residual stress have the least errors. According to the results, it can be concluded that when the ANNS are tuned carefully the modelling results are in good agreement with the experimental ones. Therefore, the ANNs can be used to predict and optimize problems if the related data are available.

## 6. REFERENCES

1. Gangaraj, S. and Farrahi, G., "Side effects of shot peening on fatigue crack initiation life", ***International Journal of Engineering-Transactions A: Basics***, Vol. 24, No. 3, (2011), 275-284.
2. Maleki, E. and Zabihollah, A., "Modeling of shot-peening effects on the surface properties of a (TiB + TiC)/Ti–6Al–4V composite employing artificial neural networks", ***Materiali in Tehnologije***, Vol. 50, No. 6, (2016), 851-860.
3. Nam, Y.-S., Jeon, U., Yoon, H.-K., Shin, B.-C. and Byun, J.-H., "Use of response surface methodology for shot peening process optimization of an aircraft structural part", ***The International Journal of Advanced Manufacturing Technology***, Vol. 87, No. 9-12, (2016), 2967-2981.
4. Farrahi, G., Lebrijn, J. and Couratin, D., "Effect of shot peening on residual stress and fatigue life of a spring steel", ***Fatigue & Fracture of Engineering Materials & Structures***, Vol. 18, No. 2, (1995), 211-220.
5. Bagherifard, S. and Guagliano, M., "Fatigue behavior of a low-alloy steel with nanostructured surface obtained by severe shot peening", ***Engineering Fracture Mechanics***, Vol. 81, (2012), 56-68.
6. Bagherifard, S., Fernandez-Pariente, I., Ghelichi, R. and Guagliano, M., "Effect of severe shot peening on microstructure and fatigue strength of cast iron", ***International Journal of Fatigue***, Vol. 65, (2014), 64-70.
7. Bagherifard, S., Slawik, S., Fernández-Pariente, I., Pauly, C., Mücklich, F. and Guagliano, M., "Nanoscale surface modification of aisi 316l stainless steel by severe shot peening", ***Materials & Design***, Vol. 102, (2016), 68-77.
8. Unal, O. and Varol, R., "Almen intensity effect on microstructure and mechanical properties of low carbon steel subjected to severe shot peening", ***Applied Surface Science***, Vol. 290, (2014), 40-47.
9. Unal, O. and Varol, R., "Surface severe plastic deformation of aisi 304 via conventional shot peening, severe shot peening and

repeening", ***Applied Surface Science***, Vol. 351, (2015), 289-295.

10. Hassani-Gangaraj, S., Moridi, A., Guagliano, M., Ghidini, A. and Boniardi, M., "The effect of nitriding, severe shot peening and their combination on the fatigue behavior and micro-structure of a low-alloy steel", ***International Journal of Fatigue***, Vol. 62, (2014), 67-76.
11. Skinner, A. and Broughton, J., "Neural networks in computational materials science: Training algorithms", ***Modelling and Simulation in Materials Science and Engineering***, Vol. 3, No. 3, (1995), 371-380.
12. Xiao, X., Liu, G., Hu, B., Zheng, X., Wang, L., Chen, S. and Ullah, A., "A comparative study on arrhenius-type constitutive equations and artificial neural network model to predict high-temperature deformation behaviour in 12Cr3WV steel", ***Computational Materials Science***, Vol. 62, (2012), 227-234.
13. Restrepo, S.E., Giraldo, S.T. and Thijsse, B.J., "Using artificial neural networks to predict grain boundary energies", ***Computational Materials Science***, Vol. 86, (2014), 170-173.
14. Sidhu, G., Bhole, S., Chen, D. and Essadiqi, E., "Determination of volume fraction of bainite in low carbon steels using artificial neural networks", ***Computational Materials Science***, Vol. 50, No. 12, (2011), 3377-3384.
15. Han, Y., Qiao, G., Sun, J. and Zou, D., "A comparative study on constitutive relationship of as-cast 904l austenitic stainless steel during hot deformation based on arrhenius-type and artificial neural network models", ***Computational Materials Science***, Vol. 67, (2013), 93-103.
16. Akbarpour, H., Mohajeri, M. and Moradi, M., "Investigation on the synthesis conditions at the interpore distance of nanoporous anodic aluminum oxide: A comparison of experimental study, artificial neural network, and multiple linear regression", ***Computational Materials Science***, Vol. 79, (2013), 75-81.
17. Velez, J.F. and Powell, G.W., "Some metallographic observations on the spalling of aisi 1060 steel by the formation of adiabatic shear bands", ***Wear***, Vol. 66, No. 3, (1981), 367-378.
18. Roy, H., Parida, N., Sivaprasad, S., Tarafder, S. and Ray, K., "Acoustic emissions during fracture toughness tests of steels exhibiting varying ductility", ***Materials Science and Engineering: A***, Vol. 486, No. 1, (2008), 562-571.
19. J443, S., Procedures for using standard shot peening almen test strip, SAE International.
20. Sun, Y., Zeng, W., Han, Y., Ma, X., Zhao, Y., Guo, P., Wang, G. and Dargusch, M.S., "Determination of the influence of processing parameters on the mechanical properties of the ti–6al–4v alloy using an artificial neural network", ***Computational Materials Science***, Vol. 60, (2012), 239-244.
21. Maleki, E. and Maleki, N., "Artificial neural network modeling of Pt/C cathode degradation in pem fuel cells", ***Journal of Electronic Materials***, Vol. 45, No. 8, (2016), 3822-3834.
22. Jahanshahi, M., Maleki, E. and Ghiami, A., "On the efficiency of artificial neural networks for plastic analysis of planar frames in comparison with genetic algorithms and ant colony systems", ***Neural Computing and Applications***, Vol. 28, No. 11, (2017), 3209-3227.
23. Zhao, J., Ding, H., Zhao, W., Huang, M., Wei, D. and Jiang, Z., "Modelling of the hot deformation behaviour of a titanium alloy using constitutive equations and artificial neural network", ***Computational Materials Science***, Vol. 92, (2014), 47-56.
24. Esmailzadeh, M. and Aghaie-Khafri, M., "Finite element and artificial neural network analysis of ECAP", ***Computational Materials Science***, Vol. 63, (2012), 127-133.
25. Benyelloul, K. and Aourag, H., "Elastic constants of austenitic stainless steel: Investigation by the first-principles calculations and the artificial neural network approach", ***Computational Materials Science***, Vol. 67, (2013), 353-358.
26. Maleki, E. and Sherafatnia, K., "Investigation of single and dual step shot peening effects on mechanical and metallurgical properties of 18crnimo7-6 steel using artificial neural network", ***Int. J. Mater. Mech. Manuf***, Vol. 4, (2016), 100-105.
27. Abendroth, M. and Kuna, M., "Determination of deformation and failure properties of ductile materials by means of the small punch test and neural networks", ***Computational Materials Science***, Vol. 28, No. 3, (2003), 633-644.
28. Maleki, N., Kashanian, S., Maleki, E. and Nazari, M., "A novel enzyme based biosensor for catechol detection in water samples using artificial neural network", ***Biochemical Engineering Journal***, Vol. 128, (2017), 1-11.
29. Elangovan, K., Narayanan, C.S. and Narayanasamy, R., "Modelling of forming limit diagram of perforated commercial pure aluminium sheets using artificial neural network", ***Computational Materials Science***, Vol. 47, No. 4, (2010), 1072-1078.
30. Maleki, E., "Artificial neural networks application for modeling of friction stir welding effects on mechanical properties of 7075-t6 aluminum alloy", in IOP Conference Series: Materials Science and Engineering, IOP Publishing. Vol. 103, (2015), 012034.
31. Maleki, E., Farrahi, G.H. and Sherafatnia, K., Application of artificial neural network to predict the effects of severe shot peening on properties of low carbon steel, in Machining, joining and modifications of advanced materials. (2016), 45-60.
32. Saitoh, H., Ochi, T. and Kubota, M., "Formation of surface nanocrystalline structure in steels by air blast shot peening", in Proceedings of the 10th international conference on shot peening, Japan., (2008), 488-493.
33. Wang, Y. and Ma, E., "Three strategies to achieve uniform tensile deformation in a nanostructured metal", ***Acta Materialia***, Vol. 52, No. 6, (2004), 1699-1709.

# Modelling of Conventional and Severe Shot Peening Influence on Properties of High Carbon Steel via Artificial Neural Network

E. Maleki[a], G. H. Farrahi[b]

[a] *Department of Mechanical Engineering, Sharif University of Technology-International Campus, Kish Island, Iran*
[b] *School of Mechanical Engineering, Sharif University of Technology, Tehran, Iran*

*P A P E R I N F O*

*Paper history:*
Received 10 June 2017
Received in revised form 05 August 2017
Accepted 08 September 2017

*Keywords*:
Artificial Neural Network
Severe Shot Peening
Residual Stress
Coverage
Almen Intensity

**چکیده**

فرایند ساچمه زنی به عنوان یکی از روش‌های تغییر شکل دائمی شدید، در بسیاری از قطعات مهندسی به منظور ارتقای خواص مکانیکی و متالورژیکی سطوح استفاده می‌شود. از طرفی دیگر، در دهه گذشته شبکه‌های عصبی مصنوعی به میزان قابل توجهی برای پیش‌بینی و بهینه‌سازی در مسائل مختلف علوم و مهندسی به کار رفته‌اند. در این مقاله، اثرات ساچمه‌زنی‌های معمولی و شدید بر روی خواص فولاد پرکربن AISI 1060 با استفاده از شبکه عصبی مصنوعی مدل سازی مقایسه شده‌اند. برای آموزش شبکه الگوریتم خطای انتشار بازگشتی به همراه داده‌های تجربی استفاده شده‌اند. نتایج آزمایشگاهی نشان می‌دهند که ساچمه‌زنی شدید اثراتی به مراتب بیشتر و بهتر نسبت به ساچمه‌زنی معمولی دارد. شبکه‌های گوناگونی با استفاده از آزمون و خطا برای یافتن ساختار بهینه‌ی شبکه آموزش داده شدند و ارزیابی شبکه توسط داده‌هایی که در فرآیند آموزش مورد استفاده قرار نگرفته بودند، صورت گرفت. عمق، میزان شدت و میزان پوشش‌دهی به عنوان ورودی و سختی، تنش پسماند و اندازه‌ی دانه‌ها به عنوان خروجی شبکه در نظر گرفته شدند. مقایسه نتایج پیش‌بینی شده و نتایج آزمایشگاهی تطابق قابل ملاحظه و قابل قبولی را در فرایند مدل سازی نشان می‌دهند.

***doi**: 10.5829/ije.2018.31.02b.24*